PROCEEDINGS A

rspa.royalsocietypublishing.org

Research

Cite this article: Estrada E. 2018 The electron density function of the Hückel (tight-binding) model. *Proc. R. Soc. A* **474**: 20170721.
http://dx.doi.org/10.1098/rspa.2017.0721

Received: 11 October 2017
Accepted: 16 January 2018

Subject Areas:
computational chemistry/graph theory

Keywords:
density matrices, sign matrix function, Euclidean distances, polycyclic aromatic compounds, graph theory, bond length alternation

Author for correspondence:
Ernesto Estrada
e-mail: ernesto.estrada@strath.ac.uk

The electron density function of the Hückel (tight-binding) model

Ernesto Estrada

Department of Mathematics and Statistics, University of Strathclyde, Glasgow G11HX, UK

EE, 0000-0002-3066-7418

The Hückel (tight-binding) molecular orbital (HMO) method has found many applications in the chemistry of alternant conjugated molecules, such as polycyclic aromatic hydrocarbons (PAHs), fullerenes and graphene-like molecules, as well as in solid-state physics. In this paper, we found analytical expressions for the electron density matrix of the HMO method in terms of odd-powers of its Hamiltonian. We prove that the HMO density matrix induces an embedding of a molecule into a high-dimensional Euclidean space in which the separation between the atoms scales very well with the bond lengths of PAHs. We extend our approach to describe a quasi-correlated tight-binding model, which quantifies the number of unpaired electrons and the distribution of effectively unpaired electrons. In this case, we found that the corresponding density matrices induce embedding of the molecules into high-dimensional Euclidean spheres where the separation between the atoms contains information about the spin–spin repulsion between them. Using our approach, we found an analytic expression which explains the bond length alternation in polyenes inside the HMO framework. We also found that spin–spin interaction explains the alternation of distances between pairs of atoms separated by two bonds in conjugated molecules.

1. Introduction

The Hückel molecular orbital (HMO) method was introduced 85 years ago [1–3] and proved to be remarkably good in describing the electron hopping on π-electronic systems [4,5] as well as in solid-state physics [6]. In molecular systems like those having conjugated π bonds, each carbon atom has an

THE ROYAL SOCIETY PUBLISHING

sp_2 hybridization which forms a trigonal planar framework characterized by its rigidity and lack of polarization [7]. The frontal overlapping of adjacent carbon atoms creates very stable σ-bonds. In addition, each carbon centre contains one hybridized p_z orbital which is perpendicular to the sp_2 plane. The lateral $p_z - p_z$ overlapping between two adjacent carbon atoms creates very labile π-bonds. Thus, it is clear from the reactivity of this molecule that a $\sigma - \pi$ separation is plausible and we can consider that our basis set consists of orbitals centred on the particular carbon atoms in such a way that there is only one orbital per spin state at each site. Then, using the second quantization approach the HMO Hamiltonian reads as

$$\hat{H} = -\sum_{ij\nu} t_{ij}\hat{c}^{\dagger}_{i\nu}\hat{c}_{j\nu}, \tag{1.1}$$

where $\hat{c}^{\dagger}_i(\hat{c}_j)$ annihilates (creates) a π-electron with spin ν in an orbital centred at the atom i, and t_{ij} is an integral which controls the hopping of a π-electron from one site i to a nearest neighbour j. The physical assumption of this model, as expressed by its Hamiltonian, is that the potential is so large that the electrons are tightly bounded to their atoms—this is the reason of the term 'tight-binding' used for these models—with only occasional hops from one atom to another.

Let us use the standard notation $t_{ii} = -\alpha_i$ and $t_{ij} = -\beta_{ij}$. Then, we can write the HMO Hamiltonian as

$$\hat{H} = \sum_{i\nu} \alpha_i \hat{c}^{\dagger}_{i\nu}\hat{c}_{i\nu} + \sum_{\langle ij\rangle\nu} \beta_{ij}\hat{c}^{\dagger}_{i\nu}\hat{c}_{j\nu}. \tag{1.2}$$

For the study of carbon-conjugated molecules, the HMO method further assumes that (i) all diagonal elements of $\hat{H}$ have the same value α, (ii) $\beta_{ij} = 0$ if the atoms i and j are not bonded, and (iii) all carbon–carbon bonds have the same strength, such that all non-zero off-diagonal elements of $\hat{H}$ have the same value β. The resulting HMO Hamiltonian is simply

$$\hat{H} = \alpha I + \beta A, \tag{1.3}$$

where I is the identity matrix, and A is the adjacency matrix whose entries are defined as $A_{ij} = 1$ if the atoms i and j are bonded, or zero otherwise.

Recently, there has been a rebirth of interest in HMO triggered by the discovery a very large carbon molecules, such as fullerenes, nanotubes and graphene [8–11], but also by the study of quantum phenomena in molecules like destructive interference [12–16]. The fundamental role of the HMO Green function in explaining the phenomenon of destructive quantum interference has been clarified by a series of papers [17–19], which has conducted an exhaustive analysis of this function from a physico-mathematical point of view [20]. The thermal Green function of the HMO method was also studied in a general graph-theory context [21] and of the quantum-harmonic oscillators [22]. Estrada & Benzi [23] have also found the structural meaning of the HMO total energy, which resulted to be a contribution from even powers of the HMO Hamiltonian. The works of Luzanov *et al.* [24–26] about a quasi-correlation tight-binding (QCTB) model of HMO type is another example of beautiful extension of the classical HMO method beyond its original horizons to account for radicaloid structure in polycyclic aromatic compounds. In his 2000 Nobel lecture 'The discovery of polyacetylene film: the dawning of an era of conducting polymers' [27] Hideki Shirakawa recognized the value of HMO in determining that 'the difference between the lengths of double and single bonds decreases with increasing the conjugation and that all the bonds tend to be of equal length in an infinitely long polyene'. This prediction is based on the known relationship between the HMO bond orders and the bond distances in these molecules.

Here, we show analytically that the HMO density matrix induces an embedding of a molecule into a Euclidean space, in such a way that the separation between the atoms in such space provides their bond distances. In this work, we use the connection between HMO and graph theory, which allows not only the numerical characterization of molecular properties, but also more importantly its conceptual understanding in terms of simple molecular concepts. In particular, we prove that the HMO density matrix can be expressed in terms of odd powers of the HMO Hamiltonian, which corresponds to the adjacency matrix of the molecular graph. We extend

our approach to consider a quasi-correlation tight-binding (QCTB) model which accounts for the unpaired electron density over the atoms of alternant hydrocarbons. Using a natural embedding of alternant molecules into Euclidean spheres induced by the QCTB density matrix, we have found important contributions of the unpaired electron repulsion to the geometry of alternant molecules, such as 1,3,5,7-octatetraene. This paper is written in a self-contained manner such that the reader can find most of the concepts and definitions used in this work without the necessity of digging into the mathematics and chemistry literature to find them.

2. Hückel molecular orbital density matrix and walks

The HMO density matrix P is the matrix whose r,s entries are defined by

$$P_{rs} = \sum_{j}^{\text{occ}} \psi_{j,r}\psi_{j,s}, \tag{2.1}$$

where $\psi_{j,r}$ is the entry of the jth eigenvector of $\hat{H}$ corresponding to the atom r and the sum is carried out over all occupied orbitals. The diagonal elements of the density matrix $P_{rr} = \sum_{j}^{\text{occ}} \psi_{j,r}^2$, corresponds to the electron density at the atom r and the non-diagonal terms correspond to one half of the bond order between the two atoms. Positive bond orders indicate *bonding* properties between the two atoms, while negative values indicate *antibonding* properties between the corresponding atoms. *No-bonding* is indicated by $P_{rs} = 0$.

Here we consider only molecules represented by non-singular HMO Hamiltonians $\hat{H}$, i.e. $\text{Re}(\lambda_j) \neq 0$ for all j. Then, the HMO density matrix function can be written as

$$P_\mu = \tfrac{1}{2}(I - \text{sgn}(\hat{H} - \mu I)), \tag{2.2}$$

where μ is a reference energy and $\text{sgn}(M)$ represents the sign matrix function of the matrix M. The sign matrix function is defined as follows [28–30]. Let $M = PJP^{-1}$ be the Jordan canonical form of the matrix M, where $J = \text{diag}(J_1, \ldots, J_k)$. Then, the sign matrix function of M is defined as

$$\text{sgn}(M) = P\,\text{sgn}(J)P^{-1}, \tag{2.3}$$

where $\text{sgn}(J) = \text{diag}(\text{sgn}(J_1), \ldots, \text{sgn}(J_k))$ and the sign of the Jordan block J_i of size p with eigenvalue λ is typically defined as

$$\text{sgn}(J_i) = \begin{cases} I_{p\times p} & \text{if } \text{Re}(\lambda) > 0, \\ -I_{p\times p} & \text{if } \text{Re}(\lambda) < 0, \\ 0_{p\times p} & \text{if } \text{Re}(\lambda) = 0. \end{cases} \tag{2.4}$$

The connection between electron density matrix and the matrix sign function is well documented (see, for instance, [31,32]). Hereafter we consider that $\hat{H} = -A$—this assumes that $\beta < 0$—and let $\mu = 0$. Then, the HMO charge-density matrix takes the form

$$P = P_0 = \tfrac{1}{2}(I + \text{sgn}(A)). \tag{2.5}$$

Now we are going to find an interpretation of the HMO density matrix in terms of walks on graphs. We start by reminding that the matrix sign function can be expressed as $\text{sgn}(M) = M(M^2)^{-1/2}$ for $\|M\| < 1$ [30]. Then we can write

$$\text{sgn}(A) = \frac{A}{\lambda_1}\left(\frac{A^2}{\lambda_1^2}\right)^{-1/2} = \frac{A}{\lambda_1}\left(I + \left(\frac{A}{\lambda_1}\right)^2 - I\right)^{-1/2} = \frac{A}{\lambda_1}(I + B)^{-1/2}, \tag{2.6}$$

where $B = (A/\lambda_1)^2 - I$ and λ_1 is the largest eigenvalue of A. Then, using the binomial theorem we can express the HMO density matrix in terms of powers of the matrix B

$$P = \frac{1}{2}\left(I + \frac{A}{\lambda_1}\sum_{k=0}^{\infty}\frac{(2k-1)!!}{(2k)!!}(-B)^k\right), \tag{2.7}$$

for which the first few terms reads as

$$P=\frac{1}{2}\left(I+\frac{A}{\lambda_1}\left(I-\frac{1}{2}\left(\frac{A^2}{\lambda_1^2}-I\right)+\frac{3}{8}\left(\frac{A^2}{\lambda_1^2}-I\right)^2-\frac{5}{16}\left(\frac{A^2}{\lambda_1^2}-I\right)^3+\cdots\right)\right). \tag{2.8}$$

By developing these terms of the power series, we arrive at the following expression for the HMO density matrix:

$$P=\frac{I}{2}+\left(\frac{1}{2}+\frac{1}{4}+\frac{3}{16}+\frac{5}{32}+\cdots\right)\frac{A}{\lambda_1}-\left(\frac{1}{4}+\frac{3}{8}+\frac{15}{32}+\cdots\right)\frac{A^3}{\lambda_1^3}$$
$$+\left(\frac{3}{16}+\frac{15}{32}+\cdots\right)\frac{A^5}{\lambda_1^5}-\left(\frac{5}{16}+\cdots\right)\frac{A^7}{\lambda_1^7}\cdots. \tag{2.9}$$

Let us now introduce the following concept. Let $G=(V,E)$ be a molecular graph with adjacency matrix A (for an introduction into the topic, see [33]). That is, we represent the hydrogen-depleted skeleton of a molecule in form of a graph, such that every carbon atom is represented by a node $i\in V$ and every covalent bond between two atoms i and j is represented by an edge $(i,j)\in E$. Then, a *walk* of length k in the graph G is a set of nodes $i_1,i_2,\ldots,i_k,i_{k+1}$ such that for all $1\leq l\leq k$, $(i_l,i_{l+1})\in E$. A *closed walk* is a walk for which $i_1=i_{k+1}$. It is known that $(A^k)_{rs}$ counts the number of walks of length k between the nodes r and s. In a similar way, $(A^k)_{rr}$ counts the number of closed walks (CW) of length k starting (and ending) at the node r [34]. Consequently, we have the following interpretation of the HMO density matrix elements:

— the HMO electron density over a given atom P_{rr} is a weighted sum of closed walks of odd length starting (and ending) at the corresponding atom;
— the HMO bond order between two atoms P_{rs} is a weighted sum of walks of odd length between the corresponding atoms.

The main conclusion of this section is that the HMO density matrix can be written on the basis of contributions coming only from odd powers of the Hamiltonian with alternant signs,

$$P=\frac{I}{2}+a_1\frac{A}{\lambda_1}-a_3\frac{A^3}{\lambda_1^3}+a_5\frac{A^5}{\lambda_1^5}-a_7\frac{A^7}{\lambda_1^7}+a_9\frac{A^9}{\lambda_1^9}-\cdots. \tag{2.10}$$

There are two unexpected findings in connection to the relationship between the density matrix and the powers of the HMO Hamiltonian. The first is that this relation is based only on odd-powers of the HMO Hamiltonian and the second is the alternation of the contributions of different powers. Let us first consider the influence of odd-powers on the diagonal and non-diagonal entries of the density matrix. If we first restrict ourselves to alternant molecules, whose graphs are bipartite, then we have the following important observations: (i) there are no closed walks of odd length starting at any atom of the molecule and (ii) every walk of odd length starting at a node p and ending at a node q encloses an alternant path. An alternant path is a path in which a double-bond alternates with a single one. As a consequence of these observations, we have that in alternant molecules the π electron density on every atom is equal to 1/2 due to the fact that $a_1=\cdots=a_n=0$ in equation (2.10). On the other hand, the bond order of a bond p,q is given by the sum of positive and negative contributions of all alternant paths connecting the two atoms. Here, the sign of the contributions plays an important role. For instance, let us consider 1,3-cyclobutadiene. In this case, the bond order of the bond 1,2 is given by the contribution a_1 due to the fact that the two atoms are connected, then there is a negative contribution coming from the coefficient a_3 due to the fact that the atoms 1 and 2 are also joint by an alternant path of length 3, which in this case involves the 4-cycle: $C_1-C_4-C_3-C_2$. It is known by the Hückel rule that rings of length $4j$ ($j=0,1,\ldots$) are destabilizing of π-electronic systems. The stabilizing contribution of the path $C_1-C_2-C_3-C_4$ to the bond C_1-C_2 comes here by counting walks of length 5, such as 1-2-3-4-3-2. Thus, in general, the contributions coming from the powers A^{4j+1} ($j=0,1,\ldots$) are positive due to the fact that they involve conjugated paths of length $4j+2$. On

the other hand, the contributions from powers A^{4j+3} ($j=0,1,\ldots$) are negative due to the fact that they involve paths of length $4j$. In the case of non-alternant molecules, the main difference is that the electron density on the atoms is no longer equal to 1/2, but it is also affected by closed walks of odd-lengths existing in those molecules. The alternation of the signs in the contributions to equation (2.10) accounts for the stability of the free radicals formed in those systems. For instance, the negative sign of a_3 indicates that the closed walks of length 3 make negative contributions to the electron charge. This is due to the fact that in a cyclobutenyl radical, there are four electrons (two from the double bond and two from the lone pair) which equals to the $4j$ ($j=0,1,\ldots$) rule. By contrast, in the cyclopentadienyl radical there are six electrons, which obeys the $4j+2$ ($j=0,1,\ldots$) rule.

Before finishing this section, we want to remark that the use of walks in understanding HMO structure and molecular properties in general has been very successful (see, for instance, [35,36]). The initial researches in the connection between powers of the HMO Hamiltonian and electronic properties of molecules were due to Rudolf Marcus in 1965 [37] and Cyrot-Lackmann in 1968 [38,39]. Further works extended these ideas to develop the so-called 'method of moments' [40–43]. More recently, it has been used in combination with modern quantum chemical methods to study inorganic molecules [44] as well as in terms of matrix functions as the one studied here (see, for instance, [45]).

3. The geometry induced by Hückel molecular orbital electron-density matrix

Let us ask the following question: How do the electron densities at the atoms and bonds of a molecule separate the corresponding atoms from each other? That is, we should expect that high electron densities at the atoms r and s, respectively, will make that the two atoms repel each other increasing their separation. On the other hand, a high electron density between the two atoms indicates that they attract each other and so decreases their separation in space. Let us then define the following quantity which captures the difference between these two competing factors

$$\delta_{rs}^2 = P_{rr} + P_{ss} - 2P_{rs}. \tag{3.1}$$

A short separation δ_{rs}^2 between the atoms r and s then depends on the fact that P_{rr} and P_{ss} are relatively small and that P_{rs} is relatively large. Let us write this expression in vector-matrix form

$$\Delta^2 = \boldsymbol{p}\cdot\mathbf{1}^{\mathrm{T}} + \mathbf{1}\cdot\boldsymbol{p}^{\mathrm{T}} - 2P, \tag{3.2}$$

where $\boldsymbol{p}=\mathrm{diag}(P)$. Let $P = V\Sigma V^{\mathrm{T}}$ be the spectral decomposition of the electron density matrix, where $V=[\boldsymbol{v}_1,\boldsymbol{v}_2,\ldots,\boldsymbol{v}_n]$ and $\Sigma=\mathrm{diag}(\sigma_j)$. Then, δ_{rs}^2 can be written as

$$\delta_{rs}^2 = \sum_{j=1}^{n} v_j^2(r)\,\mathrm{sgn}(\sigma_j) + \sum_{j=1}^{n} v_j^2(s)\,\mathrm{sgn}(\sigma_j) - 2\sum_{j=1}^{n} v_j(r)v_j(s)\,\mathrm{sgn}(\sigma_j). \tag{3.3}$$

The eigenvalues of P are either 1 or 0, each of them with multiplicity $n/2$. Then,

$$\begin{aligned}\delta_{rs}^2 &= \sum_{j=1}^{n/2}(v_j^2(r) + v_j^2(s) - 2v_j(r)v_j(s)) \\ &= \sum_{j=1}^{n}(v_j^2(r) + v_j^2(s) - 2v_j(r)v_j(s)) \qquad (3.4)\\ &= \sum_{j=1}^{n}(v_j(r) - v_j(s))^2. \qquad (3.5)\end{aligned}$$

Let $\boldsymbol{\zeta}_r = [v_1(r), v_2(r), \ldots, v_n(r)]^{\mathrm{T}}$, then we can write

$$\delta_{rs}^2 = (\boldsymbol{\zeta}_r - \boldsymbol{\zeta}_s)^{\mathrm{T}}(\boldsymbol{\zeta}_r - \boldsymbol{\zeta}_s)$$

$$= \|\boldsymbol{\zeta}_r - \boldsymbol{\zeta}_s\|^2, \tag{3.6}$$

which means that δ_{rs}^2 is a squared Euclidean distance between the atoms r and s. It is easy to see that if the adjacency matrix has spectral decomposition $A = U\Lambda U^{\mathrm{T}}$, then because $P = U\,\mathrm{sgn}(\Lambda + I)U^{\mathrm{T}}$, then we have $\delta_{rs}^2 = 1 + \sum_{j=1}^{n}(\psi_j(r) - \psi_j(s))^2\,\mathrm{sgn}(\lambda_j)$, where $\boldsymbol{\psi}_j$ and λ_j are eigenvectors and eigenvalues of A. The expression is equivalent to consider only the sum over the occupied orbitals: $\delta_{rs}^2 = 1 + \sum_{j=1}^{\mathrm{occ}}(\psi_j(r) - \psi_j(s))^2$. For a general proof of the embedding of graphs in Euclidean spaces, the reader is directed to [46].

The vector $\boldsymbol{\zeta}_r$ represents the position vector of the atom r in a Euclidean space in which the molecule is embedded. That is, the vector uniquely determines the position of the atom r in this Euclidean space which naturally emerges from the electron density properties of the molecule. If we consider two atoms r and s, then we can consider the angle between the two corresponding position vectors of these atoms in the embedding space [47]. That is,

$$\cos\theta_{rs} = \frac{\boldsymbol{\zeta}_r \cdot \boldsymbol{\zeta}_s}{\|\boldsymbol{\zeta}_r\|\|\boldsymbol{\zeta}_s\|}.$$

Note that θ_{rs} is not a bond angle. The angle α_{rst} formed by the atoms $\angle_{r,s,t}$ is related to the electron density distance by $\alpha_{rst} = (\delta_{rs} + \delta_{st} - \delta_{rt})/(2\sqrt{\delta_{rs}\delta_{st}})$. Instead, the electron density angles and distances are related via the following expression:

$$\delta_{rs}^2 = \|\boldsymbol{\zeta}_r\|^2 + \|\boldsymbol{\zeta}_s\|^2 - 2\|\boldsymbol{\zeta}_r\|\|\boldsymbol{\zeta}_s\|\cos\theta_{rs}. \tag{3.7}$$

(a) Geometric meaning of bond orders

The concept of bond order was first introduced by Coulson as the off-diagonal entries of the 'charge–bond order matrix' [48]. This quantity characterizes very well the degree of π-bonding between two atoms in a conjugated system. It is clear that this π-bond order decays with the increase of conjugation of the corresponding bonds. According to its definition based on the orbital coefficients the Coulson bond order is related to the 'degree to which the different π-orbitals have significant simultaneous (and 'left in phase') contributions from the basis orbitals of both atoms in question' [49]. As remarked by Mayer, this concept is indeed related to Lewis's shared electron concept in spite of the fact that 'there is no π-electron charge shared between the atoms' [49]. Thus, although bond order is an intuitive concept, easy to define in terms of orbital coefficients, having a different interpretation, i.e. a geometric one, can help us understanding better more complex situations in which the concept is involved. Here we give such geometric interpretation using the electron density angles defined in this work.

First, we start by observing that the length of the vector $\boldsymbol{\zeta}_r$ is $\|\boldsymbol{\zeta}_r\|^2 = P_{rr}$. Thus, the electron density angle is related to the electron density and bond order as follows:

$$\cos\theta_{rs} = \frac{P_{rs}}{\sqrt{P_{rr}P_{ss}}}. \tag{3.8}$$

Then, in conjugated alternant molecules where $P_{rr} = 1/2$ for all atoms we have

$$\cos\theta_{rs} = 2P_{rs} = \rho_{rs}, \tag{3.9}$$

where ρ_{rs} is the bond order of the corresponding bond. The angle θ_{rs} indicates the collinearity between the position vectors $\boldsymbol{\zeta}_r$ and $\boldsymbol{\zeta}_s$, such that angles close to zero indicate that both position vectors are highly collinear, which corresponds to the maximum bond order between the two atoms (note that it refers here to the π bond order which is between zero and one). On the contrary, when the angle is 90° the two position vectors are perpendicular and the bond order between the two atoms is zero. In closing, the bond order represents the collinearity between the position vectors of the corresponding atoms in the density matrix Euclidean space.

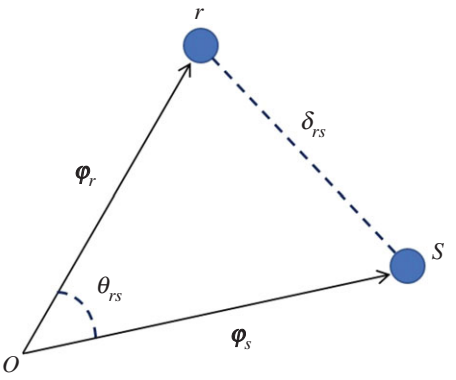

Figure 1. Illustration of the electron density distance δ_{rs} and angle θ_{rs} for two atoms *r* and *s*. The point *O* represents the centre of the coordinate system where the position vectors start. (Online version in colour.)

On the other hand, on the definition of the electron density distance, we can easily observe that

$$\rho_{rs} = 1 - \delta_{rs}^2, \tag{3.10}$$

which means that the bond order is the difference between a hypothetical interatomic distance equal to one and the actual squared electron density distance between the two atoms. Then, the maximum π bond order between the two atoms is obtained when the squared electron density distance is close to zero, and the minimum bond order is when the squared electron density distance is exactly the unity. In figure 1, we show a geometric interpretation of the electron density distances and angles in molecules.

The electron density distance is linearly related to the bond lengths in conjugated molecules, such as in polycyclic aromatic hydrocarbons (PAHs). In table 1, we report the parameters of the linear correlation observed between the electron density distances and the experimental bond distance for 18 PAHs according to the linear regression $r_{rs} = m\delta_{rs}^2 + b$, where r_{rs} is the bond length determined by X-rays crystallography. In table 1, we also give the values of the linear regression coefficient *r* and the root mean squared error (RMSE) of the regression. We also provide the statistical parameters of a general regression including all 18 PAHs. The experimental bond distances are taken from [50] and references therein. As can be seen the correlation between the electron density distances and the experimental bond lengths is remarkably good. This relationship between two Euclidean distances can be seen as a transformation of coordinates from the circum-Euclidean ones in which the electron density distances embed the molecule to the physical three-dimensional space in which the molecules exist. Then, it provides a geometric explanation to the well-known relationship between the bond orders and bond lengths due to the fact that $r_{rs} = m(1 - \rho_{rs}) + b = -m\rho_{rs} + c$.

4. Quasi-correlated tight-binding model

One of the areas in which the HMO density matrix has found new grounds of interesting applications is in the diagnostic of radicaloid states in formally closed-shell molecules. In particular, the quasi-correlated tight-binding (QCTB) model quantifies the number of unpaired electrons and the distribution of effectively unpaired electrons (EUE) over the molecule [24–26]. The theory has been successfully applied to polycyclic aromatic hydrocarbons and graphene-like molecules. Here we follow [26] in presenting this theory. The QCTB is based on a modification of the HMO Hamiltonian of bipartite molecules in the following way. The HMO Hamiltonian of a

Table 1. Fitting parameters for the bond distances as a function of bond distances of polycyclic aromatic compounds according to the linear model described in the text. *Data based on optimized structures with density functional theory at the B3LYP/6-311++G(d,p) level reported by Jones & Lin [51]. The results based on X-ray data show a poor correlation with $r \approx 0.66$. For the data used for picene, see appendix A and figure 6.

no.	name	*m*	*b*	*r*	RMSE
1	naphtalene	0.256	1.302	0.977	0.006
2	phenanthrene	0.346	1.258	0.967	0.013
3	anthracene	0.332	1.269	0.970	0.009
4	tetracene	0.368	1.254	0.981	0.008
5	triphenylene	0.332	1.274	0.979	0.008
6	chrysene	0.371	1.252	0.967	0.003
7	pyrene	0.290	1.284	0.995	0.003
8	perylene	0.379	1.249	0.995	0.002
9	1,2,5,6-dibenzanthracene	0.327	1.276	0.984	0.003
10	3,4-benzopyrene	0.381	1.254	0.948	0.013
11	dibenzo[*a*,*c*]anthracene	0.271	1.279	0.975	0.010
12	picene*	0.300	1.291	0.981	0.004
13	pentacene	0.361	1.258	0.973	0.007
14	coronene	0.224	1.315	0.992	0.004
15	quaterrylene	0.365	1.257	0.997	0.007
16	hexabenzo[*bc*,*ef*,*hi*,*kl*,*no*,*kr*]coronene	0.355	1.258	0.992	0.004
17	ovalene	0.185	1.336	0.999	0.0002
18	benzo[1,2,3-*bc*:4,5,6-*b′c′*]dicoronene	0.095	1.378	0.966	0.004
	all	0.383	1.245	0.981	0.004

bipartite molecule can be written as

$$\hat{H} = -A = -\begin{pmatrix} 0 & B \\ B^{\mathrm{T}} & 0 \end{pmatrix}, \tag{4.1}$$

where B is a block indicating the connection between starred and unstarred atoms in the molecule and 0 is an all-zeroes block. QCTB further assigns some spin up σ_1 to one of the sets of atoms, e.g. the starred ones, and spin down σ_2 to the other set, e.g. to unstarred ones. Then, the following two HMO-like Hamiltonians are written for a bipartite molecule

$$\hat{H}^{\sigma_1} = -\begin{pmatrix} -\delta I & B \\ B^{\mathrm{T}} & \delta I \end{pmatrix} \tag{4.2}$$

and

$$\hat{H}^{\sigma_2} = -\begin{pmatrix} \delta I & B \\ B^{\mathrm{T}} & -\delta I \end{pmatrix}. \tag{4.3}$$

We should note that $A = -(\hat{H}^{\sigma_1} + \hat{H}^{\sigma_2})$. Now, we obtain the respective density matrices for both Hamiltonians

$$P^{\sigma_1} = \tfrac{1}{2}(I - \mathrm{sgn}(H^{\sigma_1})) \tag{4.4}$$

and

$$P^{\sigma_2} = \tfrac{1}{2}(I - \mathrm{sgn}(H^{\sigma_2})). \tag{4.5}$$

The full charge density matrix is simply obtained by adding both spin-based density matrices

$$\begin{aligned} P_{\mathrm{QCTB}} &= P^{\sigma_1} + P^{\sigma_2} \\ &= I + A(A^2 + \delta^2 I)^{-1/2}. \end{aligned} \tag{4.6}$$

We now express the full charge density matrix as a power series of the adjacency matrix of the molecular graph,

$$\begin{aligned} P_{\mathrm{QCTB}} &= I + \frac{A}{\sqrt{\mu_1}}\left(I + \frac{B}{\mu_1} - I\right)^{-1/2} \\ &= I + \frac{A}{\sqrt{\mu_1}}(I + C)^{-1/2}, \end{aligned} \tag{4.7}$$

where $\mu_1 = \lambda_1^2 + \delta^2$, $B = A^2 + \delta^2 I$ and $C = B/\mu_1 - I = (A^2 - \lambda_1^2 I)/\mu_1$. Note that $\|C\| < 1$. Then we can expand $(I + C)^{-1/2}$ as a power series to obtain

$$P_{\mathrm{QCTB}} = I + \frac{A}{\sqrt{\mu_1}}\left(I - \frac{A^2 - \lambda_1^2 I}{2\mu_1} + \frac{3(A^2 - \lambda_1^2 I)^2}{8\mu_1^2} - \frac{5(A^2 - \lambda_1^2 I)^3}{16\mu_1^3} + \cdots\right), \tag{4.8}$$

which can be expressed in the following way:

$$\begin{aligned} P_{\mathrm{QCTB}} = I &+ \left(\frac{1}{\mu_1^{1/2}} + \frac{\lambda_1^2}{2\mu_1^{3/2}} + \frac{\lambda_1^4}{8\mu_1^{5/2}} + \frac{\lambda_1^6}{16\mu_1^{7/2}} + \cdots\right)A \\ &- \left(\frac{1}{2\mu_1^{3/2}} + \frac{\lambda_1^2}{4\mu_1^{5/2}} + \frac{3\lambda_1^4}{16\mu_1^{7/2}} + \cdots\right)A^3 \\ &+ \left(\frac{3}{8\mu_1^{5/2}} + \frac{3\lambda_1^2}{16\mu_1^{7/2}} + \cdots\right)A^5 \\ &- \left(\frac{5}{16\mu_1^{7/2}} + \cdots\right)A^7 + \cdots. \end{aligned} \tag{4.9}$$

Now, because $\mu_1 = \lambda_1^2 + \delta^2$ it is easy to see that if $\delta = 0$, expression (4.9) is identical to the HMO charge density matrix as expected. The important conclusion here is that the QCTB density matrix displays the same pattern of powers and sign alternation as the HMO density matrix previously developed here: $P = I/2 + a_1(A/\lambda_1) - a_3(A^3/\lambda_1^3) + a_5(A^5/\lambda_1^5) - a_7(A^7/\lambda_1^7) + a_9(A^9/\lambda_1^9) - \cdots$.

The most important quantity in the QCTB method is the unpaired electron density matrix P_{U} which is obtained as follows. Let us first consider the duodempotency deviation matrix $P_{\mathrm{odd}} = 2P - P^2$ [52]. Then, $P_{\mathrm{U}} = (P_{\mathrm{odd}})^2$, where $P_{\mathrm{odd}} = \delta^2(A^2 + \delta^2 I)^{-1}$. Then, using similar techniques as the ones previously developed here we express P_{U} in terms of powers of the adjacency matrix

$$\begin{aligned} P_{\mathrm{U}} &= \delta^4(A^2 + \delta^2 I)^{-2} \\ &= \left(1 + \frac{2\lambda_1}{\mu_1} + \frac{3\lambda_1^4}{\mu_1^2} + \frac{4\lambda_1^6}{\mu_1^3} + \cdots\right)I \\ &\quad - \left(\frac{2}{\mu_1} + \frac{6\lambda_1^2}{\mu_1^2} + \frac{12\lambda_1^4}{\mu_1^3} + \cdots\right)A^2 \\ &\quad + \left(\frac{3}{\mu_1^2} + \frac{4\lambda_1^2}{\mu_1^3} + \cdots\right)A^4 \\ &\quad - \left(\frac{4}{\mu_1^3} - \cdots\right)A^6 + \cdots \end{aligned} \tag{4.10}$$

This clearly indicates that the unpaired electron density matrix P_{U} depends only on even-length walks between the atoms of the molecules. The total number of unpaired electrons N_{U} is

then $Tr(P_U)$, thus

$$N_U = \left(1 + \frac{2\lambda_1}{\mu_1} + \frac{3\lambda_1^4}{\mu_1^2} + \frac{4\lambda_1^6}{\mu_1^3} + \cdots\right) n - 2\left(\frac{2}{\mu_1} + \frac{6\lambda_1^2}{\mu_1^2} + \frac{12\lambda_1^4}{\mu_1^3} + \cdots\right) m + \left(\frac{3}{\mu_1^2} - \frac{4\lambda_1^2}{\mu_1^3} - \cdots\right) \mathrm{Tr}(A^4) - \left(\frac{4}{\mu_1^3} - \cdots\right) \mathrm{Tr}(A^6) + \cdots, \tag{4.11}$$

where n and m are the number of atoms and bonds, respectively. This expression represents the count of closed walks of even length starting (and ending) at every atom in the molecule.

(a) The geometry of the quasi-correlated tight-binding matrices

We start here by noticing that the spectral radius of $A(A^2 + \delta^2 I)^{-1/2}$ is smaller than one. That is, we can see that

$$\lim_{k\to\infty} [A(A^2 + \delta^2 I)^{-1/2}]^k = 0. \tag{4.12}$$

Consequently, $\rho(A(A^2 + \delta^2 I)^{-1/2}) < 1$, where $\rho(M)$ is the spectral radius of the matrix M, and all the eigenvalues of $A(A^2 + \delta^2 I)^{-1/2}$ are inside the unit circle. This implies that P_{QCTB} is positive definite. Indeed, the P_{QCTB} matrix can be written as

$$P_{\mathrm{QCTB}} = U\left(\frac{\Lambda}{(\Lambda^2 + \delta^2 I)^{1/2}} + I\right) U^{\mathrm{T}}, \tag{4.13}$$

where U and Λ are defined by $A = U\Lambda U^{\mathrm{T}}$. We have previously proved [46] that every positive define function of the adjacency matrix produces an embedding of the corresponding graph in an $(n-1)$-dimensional Euclidean sphere. Notice that the 1-sphere is a circumference, the 2-sphere is the three-dimensional sphere and so on.

Thus, let $\tilde{P}_{rs}$ denote the r,s entry of the QCTB matrix P_{QCTB}. Then, we can define the quantity

$$\tilde{\delta}_{rs}^2 = \tilde{P}_{rr} + \tilde{P}_{ss} - 2\tilde{P}_{rs}, \tag{4.14}$$

which can be written as

$$\tilde{\delta}_{rs}^2 = \sum_{j=1}^{n} \frac{\lambda_j}{\sqrt{\lambda_j^2 + \delta^2}} (\psi_j(r) - \psi_j(s))^2. \tag{4.15}$$

In a similar way as we have proved for the HMO density matrix, it is easy to see that $\tilde{\delta}_{rs}^2$ is a square distance function between the pairs of atoms r and s.

The matrix

$$\tilde{\Delta}^2 = \mathrm{diag}(\tilde{P}) \cdot \mathbf{1}^{\mathbf{T}} + \mathbf{1} \cdot \mathrm{diag}(\tilde{P})^{\mathrm{T}} - 2\tilde{P}, \tag{4.16}$$

is also a Euclidean distance matrix. However, because the matrix $\tilde{P}$ is positive definite—notice that P is positive semidefinite—then, the matrix $\tilde{\Delta}^2$ is circum-Euclidean. This means that the atoms of a given molecule are embedded into an $(n-1)$-Euclidean sphere, where the position of the atoms is determined by the vectors

$$\boldsymbol{x}_r = \left(\frac{\Lambda}{(\Lambda^2 + \delta^2 I)^{1/2}} + I\right)^{1/2} \boldsymbol{\varphi}_r, \tag{4.17}$$

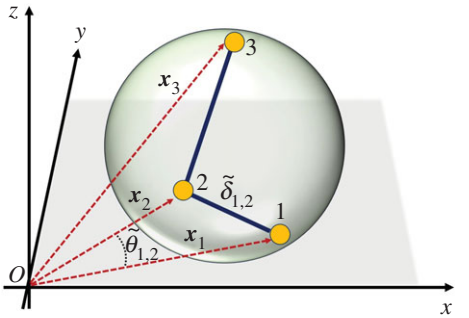

Figure 2. Schematic of the embedding of a graph with three vertices and two edges into a three-dimensional sphere according to the QCTB density distance (see text for definitions of the terms). (Online version in colour.)

where $\boldsymbol{\varphi}_r = [\psi_1(r), \psi(r), \ldots, \psi_n(r)]^{\mathrm{T}}$. Just notice that

$$\begin{aligned}\tilde{\delta}_{rs}^2 &= (\boldsymbol{\varphi}_r - \boldsymbol{\varphi}_s)^{\mathrm{T}} f(\Lambda)(\boldsymbol{\varphi}_r - \boldsymbol{\varphi}_s)\\ &= (f(\Lambda)^{1/2}(\boldsymbol{\varphi}_r - \boldsymbol{\varphi}_s))^{\mathrm{T}}(f(\Lambda)^{1/2}(\boldsymbol{\varphi}_r - \boldsymbol{\varphi}_s))\\ &= (f(\Lambda)^{1/2}\boldsymbol{\varphi}_r - f(\Lambda)^{1/2}\boldsymbol{\varphi}_s)^{\mathrm{T}}(f(\Lambda)^{1/2}\boldsymbol{\varphi}_r - f(\Lambda)^{1/2}\boldsymbol{\varphi}_s)\\ &= (\boldsymbol{x}_r - \boldsymbol{x}_s)^{\mathrm{T}}(\boldsymbol{x}_r - \boldsymbol{x}_s)\\ &= \|\boldsymbol{x}_r - \boldsymbol{x}_s\|^2, \end{aligned} \tag{4.18}$$

where $f(\Lambda) = \Lambda/(\Lambda^2 + \delta^2 I)^{1/2} + I$. This embedding is illustrated for the molecule consisting of three atoms (vertices) and two bonds (edges) in the figure 2.

By definition the matrix $P_{\mathrm{U}} = (P_{\mathrm{odd}})^2$, which implies that it is also positive define. Thus, using an analogous approach to the one previously described we can define the Euclidean distance

$$\delta_{U,rs}^2 = P_{U,rr} + P_{U,ss} - 2P_{U,rs}, \tag{4.19}$$

where $P_{U,rs}$ is the r,s entry of the matrix P_{U}. This Euclidean distance also induces an embedding of the molecule into an $(n-1)$-dimensional sphere.

5. Bond lengths alternation in polyenes

In this part of the work, we are giving an example of the importance of the new relations found here for studying the properties of conjugated alternant hydrocarbons. We have mentioned in the Introduction the remark of Shirakawa [27] about the fact that 'the difference between the lengths of double and single bonds decreases with increasing the conjugation and that all the bonds tend to be of equal length in an infinitely long polyene'. However, it is known that a Peierls distortion occurs, which produces a significant bond length alternation in infinite polyene of approximately 0.08 Å. Here we consider the electron density distance as a way to understand the bond length alternation (BLA) in linear polyenes. BLA is the topic of much research in theoretical and experimental physical chemistry [53–58]. We start by considering a long conjugated polyene having 10 000 carbon atoms. Then, we plot the electron density distances based on HMO and on QCTB for bonds in this polyene. In figure 3*a*, we plot the results for δ_{rs}^2 and in figure 3*b* for $\tilde{\delta}_{rs}^2$ for the first 5000 distances. For pairs of atoms separated at about 30 bonds from the extreme of the polyene, the differences between two adjacent bonds according to $\tilde{\delta}_{rs}^2$ is equal to zero. This means that according to the electron density distance based on the QCTB method there is no BLA for polyenes longer than 30 carbon atoms. By contrast, the electron density distance based on HMO gives small variations for adjacent bonds even at the centre of the polyene. These differences are of the order of 10^{-4} in the units of δ_{rs}^2. Thus, according to the electron density distance based on HMO there is still a perceptible BLA even for a polyene as long as 10 000 carbon atoms. Hereafter, we are going to investigate analytically the reasons for this bond (electron density) distance alternation.

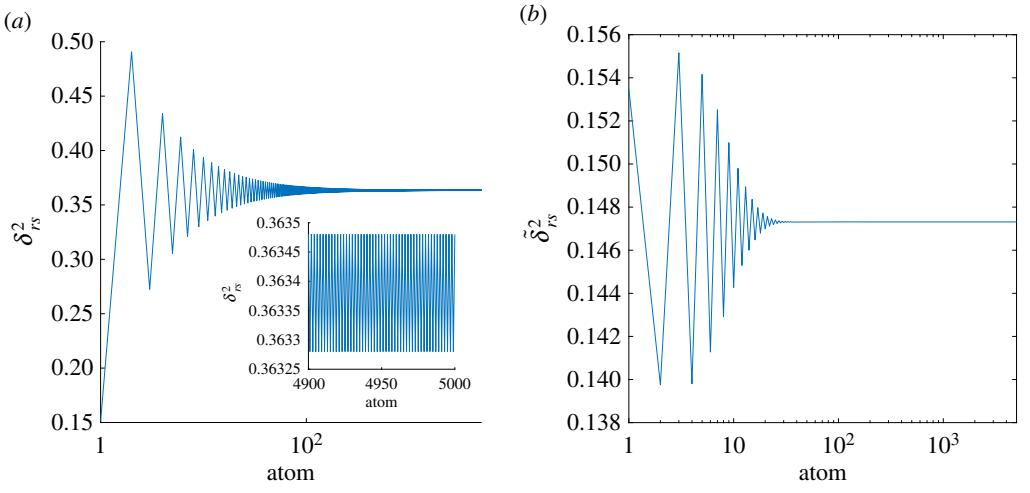

Figure 3. Value of the electron density distance δ^2_{rs} (*a*) and $\tilde{\delta}^2_{rs}$ (*b*) for the first 5000 carbon atoms of a linear polyene having 10 000 carbon atoms. The atoms are labelled from 1 to 10 000 starting from one end of the linear polyene. The inset in (*a*) corresponds to the zooming of the atoms 4900–5000 in the polyene. The plots are in logarithmic scale for *x* except for the inset where it is linear. (Online version in colour.)

Let us consider a conjugated alternant polyene with n carbon atoms, where n is an even number. Let us designate this molecule by P_n and label its atoms by $1, 2, \ldots, n$ starting from one end of the polyene. The electron density distance between any pair of atoms in P_n is given by

$$\delta^2_{rs}(P_n) = \frac{2}{(n+1)} \sum_{j=1}^{n} \left(\sin \frac{jr\pi}{n+1} - \sin \frac{js\pi}{n+1} \right)^2. \tag{5.1}$$

When $n \to \infty$ we can approximate the previous summation by the following integral, where $\vartheta = j\pi/(n+1)$:

$$\begin{aligned} \lim_{n\to\infty} \delta^2_{rs}(P_n) &= \frac{2}{\pi} \int_0^{\pi/2} (\sin \vartheta r - \sin \vartheta s)^2 \, \mathrm{d}\vartheta \\ &= \frac{2}{\pi} \left[\frac{1}{4} \left(\pi - \frac{\sin(\pi r)}{r} \right) + \frac{1}{4} \left(\pi - \frac{\sin(\pi s)}{r} \right) \right. \\ &\quad \left. - \frac{\sin(\pi(r-s)/2)}{r-s} - \frac{\cos(\pi(r+s-1)/2)}{r+s} \right] \\ &= 1 - \frac{2}{\pi} - \frac{\cos(\pi(r+s-1)/2)}{r+s}. \end{aligned} \tag{5.2}$$

In solving the previous integrals, we have used the fact that the labelling of the atoms is consecutive, such that $(r-s) = 1$. Also note that $\sin(k\pi) = 0$ for $k = 1, 2, \ldots$. This equation consists of two main parts, the term $1 - 2/\pi$ and the oscillatory term $\cos(\pi(r+s-1)/2)/(r+s)$. The second term is the one responsible for the alternation of bond (electron density) distances in the linear polyenes. When $(r+s) \to \infty$, that is when the corresponding bonds are very far from the ends of an infinite polyene, we have that all the electron density distances are equal to each other,

$$\lim_{n\to\infty} \delta^2_{rs}(P_n) \approx 1 - \frac{2}{\pi} \approx 0.3634, \tag{5.3}$$

which is the asymptote to which the values of δ^2_{rs} converges in figure 3*a*. However, it should be noticed that this convergence is very slow and the alternation is still observed in very large polyenes as the one in figure 3. In this asymptotic limit, the bond orders of each of these bonds is approximately equal to $\rho_{rs}(P_n) \approx 2/\pi \approx 0.6366$. Then, due to the relationship observed between

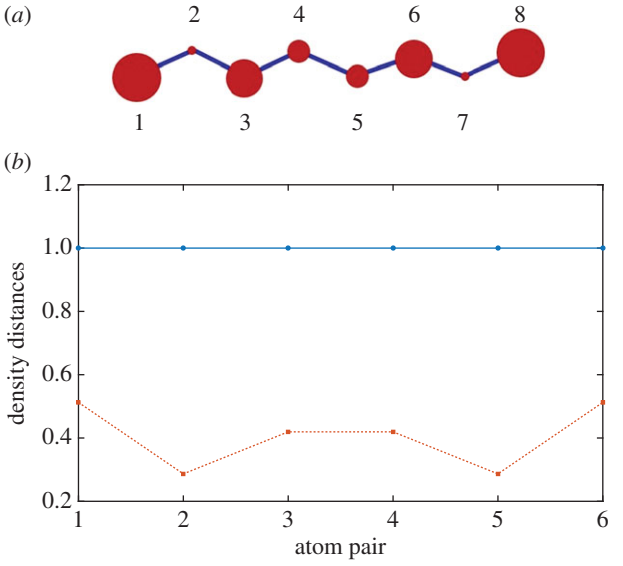

Figure 4. (*a*) Unpaired electron density in the 1,3,5,7-octatetraene according to QCTB and labelling of the atoms used here. (*b*) Plot of the calculated density distances for the different pairs of atoms separated by two bonds in 1,3,5,7-octatetraene according to the labelling provided by using HMO density matrix (solid blue line) and QCTB P_U matrix (red broken line). The labeling of the bonds in the plot (b) is in increasing order starting from (1,2), (2,3),…, and so forth. In (c) the labelling starts by (1,3), (2,4),…, and so forth. (Online version in colour.)

the electron density distance and the bond length we should expect a small alternation of the last in these molecules.

6. Distance alternation beyond bonds

Now, let us turn our attention to the interatomic distance between non-bonded pairs of atoms. We centre our analysis on the Euclidean distance $\delta^2_{U,rs}$, which takes into account the radicaloid structure of molecules. Typically, there are not two radicaloids in contiguous atoms. Thus, the radicaloid structure of a molecule should not affect significantly the bond lengths in molecules. However, the same is not true if we consider interatomic distances for non-bonded pairs of atoms. In particular, pairs of atoms separated by two consecutive bonds may display relatively large unpaired electron densities on them. Such unpaired electron densities must affect the interaction between such pairs of atoms by increasing their inter-atomic distances. To illustrate this phenomenon, we select the molecule of 1,3,5,7-octatetraene (figure 4*a*) for which crystallographic information exists about its structure.

In figure 4*b*, we plot the Euclidean distances between the pairs of atoms separated by two bonds, i.e. (1,3), (2,4) and (3,5), based on the HMO density matrix (continuous blue line) and on the P_U matrix. As can be seen the difference between the two approaches is very significant. While the HMO density matrix predicts exactly the same distance for all pairs of atoms separated by two bonds, the P_U matrix accounts for the differences in the interatomic distance expected to be produced by unpaired electron–electron interactions. In the tight-binding context, the π-electrons over each atom has either spin up or down in an alternant way. That is, if the spin on atom 1 is up (down) the spin on atom 2 is down (up) and that on atom 3 is again up (down). Thus, it is expected that if the density of unpaired electrons at atoms 1 and 3 is relatively large, then a spin-spin repulsion should separate more the pair of alternant atoms in the octatetraene molecule. As a way of confirming this prediction, we consider the interatomic distances between alternant pairs of atoms obtained by X-rays crystallography [59]. In table 2, we give the values of the distance for the pairs of atoms (1,3), (2,4) and (3,5). We also provide the values of the HMO and QCTB

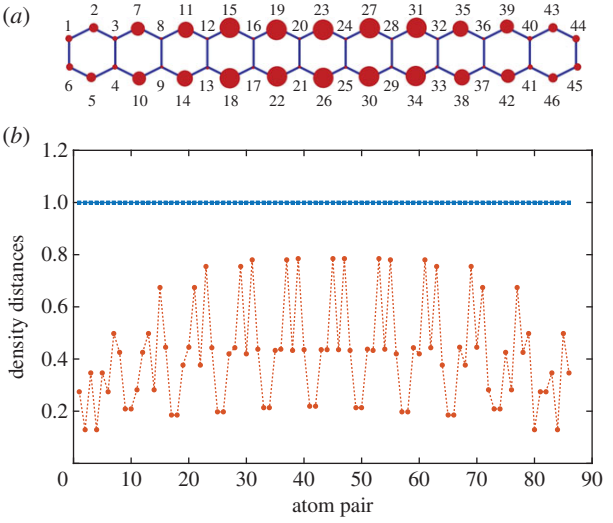

Figure 5. (*a*) Unpaired electron density in the undecacene according to QCTB and labelling of the atoms used here. (*b*) Plot of the calculated density distances for the different pairs of atoms separated by two bonds in acene according to the labelling provided by using HMO density matrix (solid blue line) and QCTB P_U matrix (red broken line). In (*b*), the labelling starts by (1,3), (2,4),…,(44,46), (1,5), (2,6), and so forth. (Online version in colour.)

Table 2. Interatomic distances between pairs of atoms separated by 2 bonds in 1,3,5,7-octatetraene according to experimental results [59], HMO and QCTB (this work) calculations.

method	$d_{1,3}$	$d_{2,4}$	$d_{3,5}$
Exp.	2.469	2.466	2.468
HMO-δ	1.000	1.000	1.000
QCTB-$\tilde{\delta}$	0.512	0.2867	0.4194

distances based on the respective density matrices. Obviously, HMO does not produce any trend as it predicts that all interatomic distances for alternant atoms are equal to the unity. However, the distance based on the P_U matrix perfectly accounts for the trend observed experimentally indicating a clear increase in the separation of atoms 1 and 3 due to the large unpaired electron densities at both atoms. The distance between atoms 2 and 4 is predicted correctly to be the shortest ones of the three and the pair 3,5 still shows certain elongation due to the unpaired electron densities. This phenomenon of bond elongation due to unpaired electrons interaction was first discovered in [60]. It is plausible that quantum mechanical calculations using spin-unrestricted DFT with proper initial guesses for the spin-polarization reproduces this spin–spin repulsion and elongation of the corresponding interatomic distance. So far, such calculations have not been reported and it is remarkable that it has been described here by using relatively simple geometric parameters from the QCTB density matrix.

Similar results are also obtained for other molecules when they are treated at the HMO or QCTB levels. For instance, in figure 5 we illustrate the results for the undecacene molecule where it can be seen that HMO predicts the same separation between every pair of alternant atoms but QCTB corrects these results and produces the expected alternation in the distances due to the interaction between unpaired electron densities with the same spin on alternant atoms.

7. Conclusion

It seems curious that 85 years after Hückel introduced the HMO method we are still discovering new edges of this method at the fundamental level. We have mentioned in the Introduction

a few recent theoretical advances in HMO theory related to Green's function, total π energy and QCTB. Here we continue with this set of expansions of the HMO method and have found analytically that the charge-electron density matrix of this method can be expressed in terms of odd powers of the HMO Hamiltonian. Consequently, both the charge density and bond orders can be expressed in terms of contributions from the different substructures forming a given molecule. In addition, we have defined Euclidean distances that naturally emerges from the electron hopping in molecules according to the description provided by the HMO method. We have extended our finding to the QCTB method of Luzanov *et al.* and have found important contributions of the unpaired electron repulsion between alternant atoms to the geometry of alternant molecules. Using our current approach we have found analytically an expression that explains the bond length alternation in linear polyenes and how it vanishes for infinitely long polyenes.

We would like to close this work by remarking what Kutzelnigg stressed in his paper entitled 'What I like about Hückel theory', which was also remarked by Luzanov *et al.*: 'We come to optimistic conclusions as to the further role of the HMO model, not as an approximation for the solution of the Schrödinger equation, but as a way towards the understanding of some aspects of the Chemical Bond'. We believe that the previously mentioned papers and the current one contribute to this goal of keeping in very good health the HMO method beyond its 85 anniversary.

Data accessibility. This work does not have any experimental data.
Competing interests. I declare I have no competing interests.
Funding. This work has no funding source associated to it.
Acknowledgements. The author thanks the Royal Society of London for a Wolfson Research Merit Award.

Appendix A

Data used for picene in table 1 (figure 6).

bond	X-rays	B3LYP/6-311++G(d,p)[1]	HMO-δ	bond	X-rays	B3LYP/6-311++G(d,p)[1]	HMO-δ
a	1.429	1.45	0.7121	h	1.367	1.38	0.5382
b	1.388	1.42	0.6609	i	1.366	1.41	0.6172
c	1.412	1.43	0.6841	j	1.409	1.38	0.5432
d	1.367	1.37	0.4915	k	1.394	1.42	0.6438
e	1.410	1.43	0.6953	l	1.469	1.45	0.7275
f	1.414	1.42	0.6801	m	1.430	1.42	0.6675
g	1.414	1.41	0.6554	n	1.406	1.37	0.5174

[1]From reference [51].

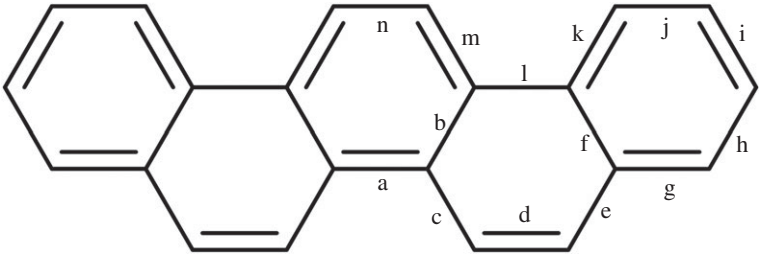

Figure 6. Labelling of the bonds in picene.

References

1. Hückel E. 1931 Quantentheoretische beiträge zum benzolproblem. I. Die Elektronenkonfiguration des Benzols und werwandter Verbindungen. *Z. Phys.* **70**, 204–286. (doi:10.1007/BF01339530)
2. Hückel E. 1931 Quantentheoretische Beiträge zum Bezolproblem. II. Quantentheorie der induzierten Polaritäten. *Z. Phys. Chem.* **72**, 310–337.
3. Hückel E. 1932 Quantentheoretische Beiträge zum Problem der aromatischen und ungesättigten Verbindungen. III. *Z. Phys. Chem.* **76**, 628–648. (doi:10.1007/BF01341936)
4. Heilbronner E, Bock H. 1976 *The HMO-model and its application*. London, UK: Wiley.
5. Coulson CA, O'Leary B, Mallion RB. 1978 *Hückel theory for organic chemists*. London, UK: Academic Press.
6. Ashcroft NW, Mermin ND. 1981 *Solid state physics*. Philadelphia, PA: Saunders College.
7. Streitwieser A. 1961 *Molecular orbital theory for organic chemists*. New York, NY: Wiley.
8. Setton R, Bernier P, Lefrant S (eds). 2002 *Carbon molecules and materials*. Boca Raton, FL: CRC Press.
9. Hirsch A. 2010 The era of carbon allotropes. *Nature Mat.* **9**, 868–871. (doi:10.1038/nmat2885)
10. Falcao EHL, Wudl F. 2007 Carbon allotropes: beyond graphite and diamond. *J. Chem. Tech. Biotech.* **82**, 524–531. (doi:10.1002/jctb.1693)
11. Allen MJ, Tung VC, Kaner RB. 2009 Honeycomb carbon: a review of graphene. *Chem. Rev.* **110**, 132–145. (doi:10.1021/cr900070d)
12. Kazunari Y, Tada T, Staykov A. 2008 Orbital views of the electron transport in molecular devices. *J. Am. Chem. Soc.* **130**, 9406–9413. (doi:10.1021/ja800638t)
13. Solomon GC, Andrews DQ, Hansen T, Goldsmith RH, Wasielewski MR, Van Duyne RP, Ratner MA. 2008 Understanding quantum interference in coherent molecular conduction. *J. Chem. Phys.* **129**, 054701. (doi:10.1063/1.2958275)
14. Markussen T, Stadler R, Thygesen KS. 2010 The relation between structure and quantum interference in single molecule junctions. *Nano Lett.* **10**, 4260–4265. (doi:10.1021/nl101688a)
15. Tsuji Y, Hoffmann R. 2014 Frontier orbital control of molecular conductance and its switching. *Angew. Chem. Int. Ed.* **53**, 4093–4097. (doi:10.1002/anie.201311134)
16. Guedon CM, Valkenier H, Markussen T, Thygesen KS, Hummelen JC, Van Der Molen SJ. 2012 Observation of quantum interference in molecular charge transport. *Nature Nanotech.* **7**, 305–309. (doi:10.1038/nnano.2012.37)
17. Markussen T, Stadler R, Thygesen KS. 2011 Graphical prediction of quantum interference-induced transmission nodes in functionalized organic molecules. *Phys. Chem. Chem. Phys.* **13**, 14311–14317. (doi:10.1039/c1cp20924h)
18. Tsuji Y, Hoffmann R, Movassagh R, Datta S. 2014 Quantum interference in polyenes. *J. Chem. Phys.* **141**, 224311. (doi:10.1063/1.4903043)
19. Tsuji Y, Yoshizawa K. 2017 Frontier orbital perspective for quantum interference in alternant and nonalternant hydrocarbons. *J. Phys. Chem. C* **121**, 9621–9626. (doi:10.1021/acs.jpcc.7b02274)
20. Movassagh R, Strang G, Tsuji Y, Hoffmann R. 2017 The Green's function for the Hückel (tight binding) model. *J. Math. Phys.* **58**, 033505. (doi:10.1063/1.4977080)
21. Estrada E, Hatano N. 2007 Statistical-mechanical approach to subgraph centrality in complex networks. *Chem. Phys. Lett.* **439**, 247–251. (doi:10.1016/j.cplett.2007.03.098)
22. Estrada E, Hatano N, Benzi M. 2012 The physics of communicability in complex networks. *Phys. Rep.* **514**, 89–119. (doi:10.1016/j.physrep.2012.01.006)
23. Estrada E, Benzi M. 2017 What is the meaning of the graph energy after all? *Discr. Appl. Math.* **230**, 71–77. (doi:10.1016/j.dam.2017.06.007)
24. Luzanov AV. 2016 Effectively unpaired electrons for singlet states: from diatomics to graphene nanoclusters. In *Practical aspects of computational chemistry IV* (eds J Leszczynski, MK Shukla), pp. 151–206. Boston, MA: Springer.
25. Luzanov AV. 2014 Effectively unpaired electrons in bipartite lattices within the generalized tight-binding approximation: application to graphene nanoflakes. *Funct. Mat.* **21**, 437–447. (doi:10.15407/fm21.04.437)
26. Luzanov AV, Plasser F, Das A, Lischka H. 2017 Evaluation of the quasi correlated tight-binding (QCTB) model for describing polyradical character in polycyclic hydrocarbons. *J. Chem. Phys.* **146**, 064106. (doi:10.1063/1.4975196)

27. Shirakawa H. 2001 The discovery of polyacetylene film–the dawning of an era of conducting polymers. *Curr. Appl. Phys.* **1**, 281–286. (doi:10.1016/S1567-1739(01)00052-9)
28. Kenney CS, Laub AJ. 1995 The matrix sign function. *IEEE Trans. Autom. Cont.* **40**, 1330–1348. (doi:10.1109/9.402226)
29. Stickel EU. 1991 Separating eigenvalues using the matrix sign function. *Lin. Algebra Appl.* **148**, 75–88. (doi:10.1016/0024-3795(91)90087-D)
30. Higham NJ. 1994 The matrix sign decomposition and its relation to the polar decomposition. *Lin. Algebra Appl.* **212**, 3–20. (doi:10.1016/0024-3795(94)90393-X)
31. Németh K, Scuseria GE. 2000 Linear scaling density matrix search based on sign matrices. *J. Chem. Phys.* **113**, 6035–6041. (doi:10.1063/1.1308546)
32. Beylkin G, Coult N, Mohlenkamp MJ. 1999 Fast spectral projection algorithms for density-matrix computations. *J. Comput. Phys.* **152**, 32–54. (doi:10.1006/jcph.1999.6215)
33. Gutman I, Polansky OE. 2012 *Mathematical concepts in organic chemistry*. Berlin, Germany: Springer Science & Business Media.
34. Cvetković DM, Rowlinson P, Simic S. 1997 *Eigenspaces of graphs*. Cambridge, UK: Cambridge University Press.
35. Estrada E, Uriarte E. 2001 Recent advances on the role of topological indices in drug discovery research. *Curr. Med. Chem.* **8**, 1699–1714. (doi:10.2174/0929867013371743)
36. Estrada E. 2008 Quantum-chemical foundations of the topological substructural molecular design. *J. Phys. Chem. A* **112**, 5208–5217. (doi:10.1021/jp8010712)
37. Marcus RA. 1965 Additivity of heats of combustion, LCAO resonance energies, and bond orders of conformal sets of conjugated compounds. *J. Chem. Phys.* **43**, 2643–2654. (doi:10.1063/1.1697189)
38. Cyrot-Lackmann F. 1968 Sur le calcul de la cohésion et de la tension superficielle des métaux de transition par une méthode de liaisons fortes. *J. Phys. Chem. Sol.* **29**, 1235–1243. (doi:10.1016/0022-3697(68)90216-3)
39. Gaspard JP, Cyrot-Lackmann F. 1973 Density of states from moments. Application to the impurity band. *J. Phys. C: Sol. Stat. Phys.* **6**, 3077–3096. (doi:10.1088/0022-3719/6/21/012)
40. Gutman I, Trinajstić N. 1972 Graph theory and molecular orbitals. Total φ-electron energy of alternant hydrocarbons. *Chem. Phys. Lett.* **17**, 535–538. (doi:10.1016/0009-2614(72)85099-1)
41. Jiang Y, Tang A, Hoffmann R. 1984 Evaluation of moments and their application in Hückel molecular orbital theory. *Theoret. Chim. Acta* **66**, 183–192. (doi:10.1007/BF00549668)
42. Burdett JK. 1995 *Chemical bonding in solids*. Oxford, UK: Oxford University Press.
43. Pettifor DG. 1995 *Bonding and structure of molecules and solids*. Oxford, UK: Oxford University Press.
44. Stacey TE, Fredrickson DC. 2012 Perceiving molecular themes in the structures bonding of intermetallic phases: the role of Hückel theory in an ab initio era. *Dalton Trans.* **41**, 7801–7813. (doi:10.1039/c2dt30298e)
45. Estrada E, Higham DJ. 2010 Network properties revealed through matrix functions. *SIAM Rev.* **52**, 696–714. (doi:10.1137/090761070)
46. Estrada E, Sanchez-Lirola MG, de la Pena JA. 2014 Hyperspherical embedding of graphs and networks in communicability spaces. *Discr. Appl. Math.* **176**, 53–77. (doi:10.1016/j.dam.2013.05.032)
47. Estrada E, Hatano N. 2016 Communicability angle and the spatial efficiency of networks. *SIAM Rev.* **58**, 692–715. (doi:10.1137/141000555)
48. Coulson CA. 1939 The electronic structure of some polyenes and aromatic molecules. VII. Bonds of fractional order by the molecular orbital method. *Proc. R. Soc. Lond. A* **169**, 413–428. (doi:10.1098/rspa.1939.0006)
49. Mayer I. 2007 Bond order and valence indices: a personal account. *J. Comput. Chem.* **28**, 204–221. (doi:10.1002/jcc.20494)
50. Kiralj R, Ferreira MMC. 2002 Predicting bond lengths in planar benzenoid polycyclic aromatic hydrocarbons: a chemometric approach. *J. Chem. Inf. Compu. Sci.* **42**, 508–523. (doi:10.1021/ci010063g)
51. Jones L, Lin L. 2017 An *in silico* study on the isomers of pentacene: the case for air-stable and alternative $C_{22}H_{14}$ acenes for organic electronics. *J. Phys. Chem. A* **121**, 2804–2813. (doi:10.1021/acs.jpca.6b11770)
52. Takatsuka K, Fueno T, Yamaguchi K. 1978 Distribution of odd electrons in ground-state molecules. *Theor. Chim. Acta* **48**, 175–183. (doi:10.1007/BF00549017)

53. Longuet-Higgins HC, Salem L. 1959 The alternation of bond lengths in long conjugated chain molecules. *Proc. R. Soc. Lond. A* **251**, 172–185. (doi:10.1098/rspa.1959.0100)
54. Su W, Schrieffer JR, Heeger AJ. 1979 Solitons in polyacetylene. *Phys. Rev. Lett.* **42**, 1698–1701. (doi:10.1103/PhysRevLett.42.1698)
55. Wu CQ, Sun X, Nasu K. 1987 Electron correlation and bond alternation in polymers. *Phys. Rev. Lett.* **59**, 831–834. (doi:10.1103/PhysRevLett.59.831)
56. Brédas JL, Heeger AJ. 1989 Comment on "Electron correlation and bond alternation in polymers". *Phys. Rev. Lett.* **63**, 2534. (doi:10.1103/PhysRevLett.63.2534)
57. Capponi S, Guihéry N, Malrieu JP, Miguel B, Poilblanc D. 1996 Bond alternation of polyacetylene as a spin-Peierls distortion. *Chem. Phys. Lett.* **255**, 238–243. (doi:10.1016/0009-2614(96)00350-8)
58. Körzdörfer T, Parrish RM, Sears JS, Sherrill CD, Brédas JL. 2012 On the relationship between bond-length alternation and many-electron self-interaction error. *J. Chem. Phys.* **137**, 124305. (doi:10.1063/1.4752431)
59. Baughman RH, Kohler BE, Levy IJ, Spangler C. 1985 The crystal structure of *trans*, *trans*-1,3,5,7-octatetraene as a model for fully-ordered *trans*-polyacetylene. *Synth. Met.* **11**, 37–52. (doi:10.1016/0379-6779(85)90172-9)
60. Estrada E, Benzi M. 2013 Atomic displacements due to Spin-Spin repulsion in conjugated alternant hydrocarbons. *Chem. Phys. Lett.* **568-569**, 184–189. (doi:10.1016/j.cplett.2013.03.021)